8-5

Passive specular surface measurements from virtual images of pattern boards

Kazuya Nagamine, Yu Suzuki and Minoru Ito
Kogakuin University
〒163-8677 1-24-2 Nishi-Shinjuku, Shinjuku-ku, Tokyo
ito@ee.kogakuin.ac.jp

Abstract

This paper describes a new approach for passive measurements of specular surfaces, in which the range and shape of specular surfaces are obtained from virtual images of pattern boards taken by the camera. In the approach, structured patterns displayed on two boards are acquired with a camera through the specular surface and each reflection point on the object is located geometrically using the triangulation principle without any prior knowledge of the coordinates of other reflection points. This feature enables us to obtain a high spatial resolution of detection with a high accuracy.

1   Introduction

Many measurement methods using laser light projection have been proposed. Nakagawa et al. scanned with a spotlight to detect solder surfaces [1]. Sanderson et al. and Nayer et al. proposed the structured pattern highlight analysis [2,3], where the light source array is moved around the object and changes in highlight distributions are analyzed. Kuroda et al. project a slit of light onto a specular surface and the object shape is restored from acquired images [4]. Miyake et al. calculate the object shape after detecting reflecting angles of LED projection light [5]. In another approach, the distortion of images acquired for the lattice pattern projection is observed and analyzed [6]. All of these techniques can be categorized as active methods for specular surface measurements. Such active methods require laser light scans and camera rotation, which may reduce the spatial resolution.

Some passive approaches have also been reported. Ye et al. observe the virtual image of a coded lattice pattern through the specular surface [7]. They obtain the normal direction distribution on the surface and then calculate the surface shape from the distribution under the assumption that the reflection on the reference surface is set beforehand. The light source must be set far from the surface to get high accuracy. Nishimura et al. used a light source with an M configuration pattern [8]. Wang et al. and Yamamoto et al. proposed an approach where the coded pattern is observed by the camera and the reference surface for calculating the normal direction at each reflection point is corrected using the known normal direction at the nearest reflection position [9,10]. This is a good idea, however, measurement errors may accumulate as the distance increases between the reflection point and the initial position on the object surface, whose coordinates must be exactly calibrated beforehand. Our colleagues, Oshima et

al., proposed a theory where both the position and normal direction at each reflection point are detected individually by resolving the differential equation without any prior knowledge [11]. Savarese et al. derive first to third order derivatives to locate the surface shape. They used the regular grid and triangular patterns as a calibrated scene [12]. In these two approaches, it seems that the robustness to noise and distortion in images is not high enough.

On the other hand, approaches for surface shape detection using images acquired from various viewpoints have been reported. Chin et al. and Blake eliminate highlight components from the images taken from some viewpoints to extract diffusion components from the images [13,14]. Bhat et al. eliminate highlight components with the surface roughness parameter known beforehand [15]. Oren et al. proposed the idea of taking virtual images of reference patterns by rotating the camera around the object [16]. Changes in pattern positions observed in images are considered in the analysis for restoration of the surface shape. In their approach, reference patterns should be set very far from the object so that the light incident to the object can be assumed to be parallel.

Normal direction detection using dependence of the polarization rotation angle on the light incident angle has been tried by Koshikawa et al. [17] and Wolff et al. [18]. The reflectance ratio must be known beforehand and the reflection point cannot be directly obtained.

In this paper, a new passive approach is proposed where structured patterns displayed on two boards are taken with a camera through the specular surface and each reflection point on the object is located geometrically by means of the triangulation principle without any prior knowledge of the coordinates of other reflection points.

2   Principle

In our approach, structured patterns on two boards are acquired with a camera, and both the position and the normal direction at each reflection point on the object are calculated directly using the triangulation principle. Figure 1 shows the principle of our technique for surface measurements of specular objects such as a mirror. The principal point of the camera lens is set at the origin of the coordinate system. One pattern board, P_1, is set along the x-axis and the other board, P_2, is located at distance t from board P_1. The structured pattern is displayed on both boards. First, the virtual image of board P_1 is acquired with the camera and then, on the pattern, the position

matching each camera pixel is located. The same procedure is performed for board P_2. Let matches on the boards corresponding to common image pixel position i be p_1 and p_2 as depicted in Fig.1. The light beam going through both p_1 and p_2 is given by

$$y = \frac{t}{s_2 - s_1}(x - s_1) \quad , \tag{1}$$

where s_1 and s_2 are the x-coordinates of p_1 and p_2. After the light is reflected at point A, it passes through the lens principal point and is incident to image point i. This reflected light beam is given by

$$y = -\frac{L}{\eta(i_x - i_0)}x \quad , \tag{2}$$

where L is the optical axis length, i_x the image point, i_0 the optical axis point coordinate, and η the conversion parameter relating a pixel of the image to real image size on the image sensor. The position of point A is determined as the intersection of the trajectory from p_2 to p_1 given by (1) and that from the lens principal point to the image point given by (2).

Thus, each reflection point on the object is located geometrically using the triangulation principle.
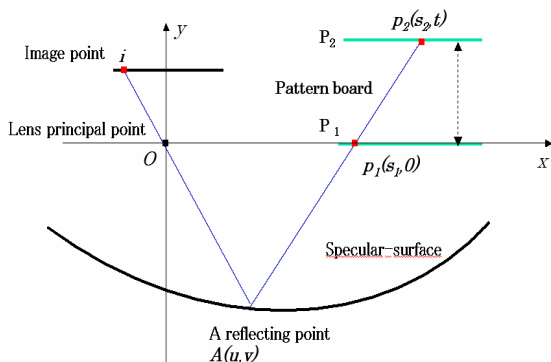

Figure 1.   Measurement principle

3   Correspondence Problem

In the conventional method for determining the correspondence between the camera image and the reference pattern, the local brightness distribution for each pixel in the image is compared with that of the reference pattern and the image position having the highest similarity is found. When an LCD board is used as the reference pattern and a camera with the sensor array such as a CCD is used, a Moire pattern may appear in the camera image. It is sometimes strong, depending on the camera and board configurations, and the output signal at each pixel from the camera is not necessarily proportional to the brightness at the corresponding position on the LCD board. For this reason, conventional techniques for finding the correspondence between the board pattern and the image based on the similarity of the brightness can hardly be applied. To overcome this problem, we use a phase shift technique. Structured patterns of the triangle saw-wave are displayed on the board. Figure 2 shows an example of

the patterns. The patterns are acquired with the camera as the phase of the wave is repetitively changed from 0 to 2π with the spacing of 1/15 period. As the phase of the pattern is changed, the brightness at each pixel changes with the function of the triangular saw-wave. The change is approximated to a polynomial equation and the phase with local maximum at each camera pixel is obtained from 15 images. The position on the board with the same phase value as that for each pixel is determined as the match to the pixel.   In this way, the correspondence between the pattern and the camera image can easily be found without any influence of the Moire effect. Figure 3 shows an example of correspondence results.

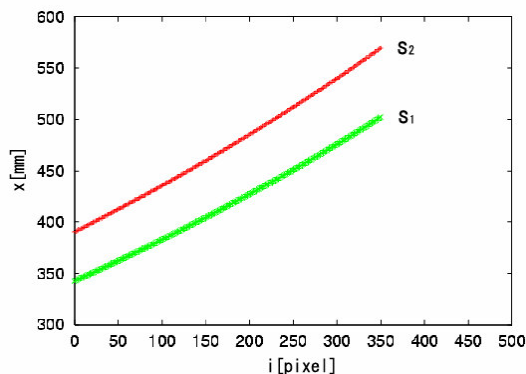Figure 2.   The pattern displayed on the pattern board.

Figure 3.   An example of the correspondence results.

4   Experiments

A camera with the lens focal length of 25 mm was used in experiments.   The camera position and direction were adjusted so that as wide a view of the pattern boards as possible could be taken, and then the camera was calibrated just before the measurement. A 3x3 spatial filtering was applied to the acquired images to reduce noise in them.

Figure 4 shows detection results for a flat mirror set 245 mm from the x-axis, where (u,v) are the coordinates of reflection points.   The principal point of the camera is (-51.1,34.0) and the orientation $\tan\theta$ is -0.980. The thin broken line is the true reflecting surface estimated from the mechanical setting of the mirror. It is clear that the position and shape are almost exactly detected. Figure 5 shows the result in the Fig.4 partially enlarged. The dominant errors with a repetitive change are quantization ones, due to digitalization in the LCD display and image acquisition.   They are probably dependent on the spacing of image sensor elements and that of the luminous elements

of the pattern board. The average of errors of the measured reflecting points from the true distribution is about 0.2 mm, and the standard deviation is about 0.31 mm. The order of quantization errors is estimated to be ±0.7 mm. Figure 6 shows the normal direction distribution on the surface. The thin broken line is the true distribution. The errors are within ±0.1 degree and are mostly due to quantization.
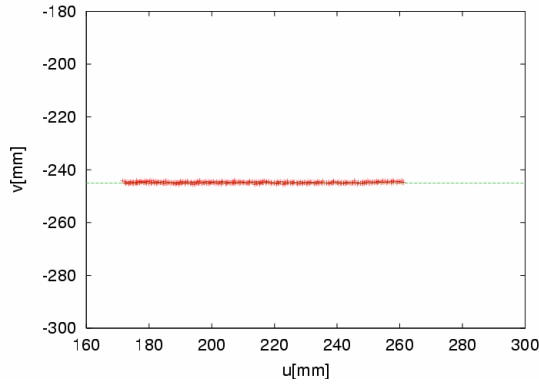

Figure 4.   Detected results for the flat mirror.
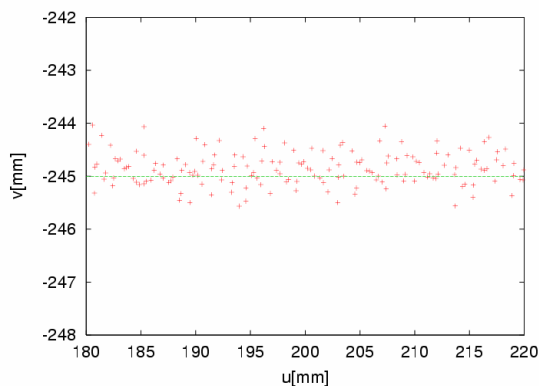

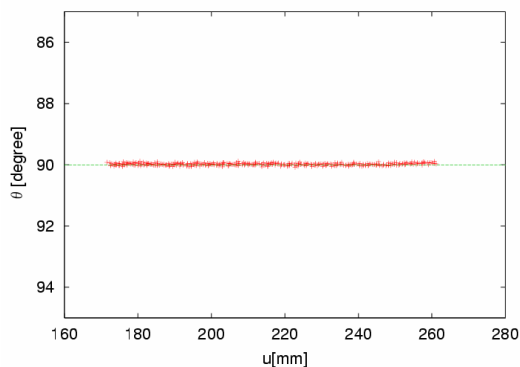Figure 5.   The result from Fig.4 partially enlarged.

Figure 6. The normal direction distribution on the
Surface.

Detected distributions of reflecting surface positions for a curved mirror are shown in Fig. 7. The radius of the mirror is 304.8 mm. The thin broken line shows the reflecting position distribution evaluated by considering the

true shape and mechanical setting of the object. The principal position of the camera is (-18.55,3.70) and the orientation tan θ is -0.986. The shape of the surface observed almost perfectly agrees with the broken line. Figure 8 shows the display in Fig.7 partially enlarged. The standard deviation is ±0.08 mm. The orders of dominant quantization errors and variation errors are estimated to be ±0.3~0.5 mm and ±0.5 mm, respectively. They tend to decrease as the position becomes farther from the center of the mirror. Figure 8 shows the normal direction distribution on the surface. It is clear that the direction angle changes linearly to the reflecting position coordinate.
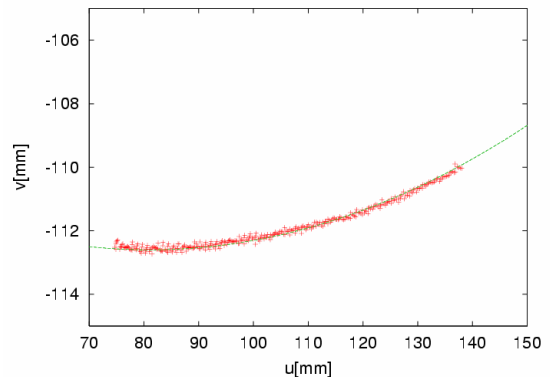

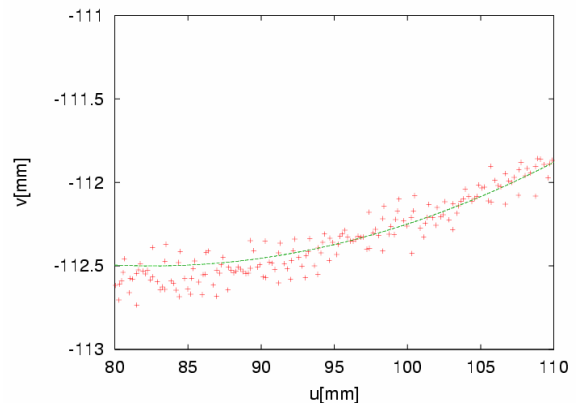Figure 7.   The detection distribution of the curved mirror surface
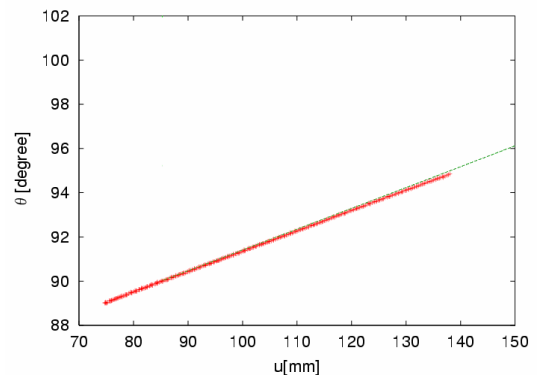

Figure 8.   The display in Fig.7 partially enlarged.

Figure 9. The normal direction distribution of the surface.

247

5 Discussion

The quantization errors appeared dominantly in the experimental results. They are caused by digitalization in the LCD display and image acquisition as mentioned in section 4. The dot pitch of the LCD display board used in experiments was 0.29 mm and the spacing of image sensor elements in the camera used was 0.02 mm. Here, let's estimate the order of the quantization errors using Fig.10 where J depicts the intersection between the beam trajectory from the pattern board to the surface and that incident to the camera after reflecting at the surface. The position of J changes from B to F. BC is given by

$$BC = \frac{2}{t}\left(\frac{t}{2}+h\right)DE \ , \qquad (3)$$

where t is the distance between two pattern board positions and h the distance from the mirror surface to the pattern board. When the dot pitch of the board is 0.3 mm, t is 60 mm and h is 260 mm, BC is calculated to be 2.9 mm. If the camera direction is 45 degrees, GF is about 1.45 mm. That is, the quantization error is estimated to be about $\pm$ 0.7mm.

The order of estimated quantization errors for the detection of the flat mirror in the experiment mentioned in the previous section is about ±0.8 mm, which is almost equal to that in the experiments. If a large spatial filter is applied to the input images, many of the step-wise dominant errors due to the quantization should be eliminated. However, the large filtering may greatly reduces the spatial resolution. Eliminating the quantization errors requires a display with a smaller dot pitch and a camera with small spacing sensor elements. This requirement will be satisfied in future because a LCD board with the smaller dot pitch and a camera with high-density sensor elements have appeared on the market.
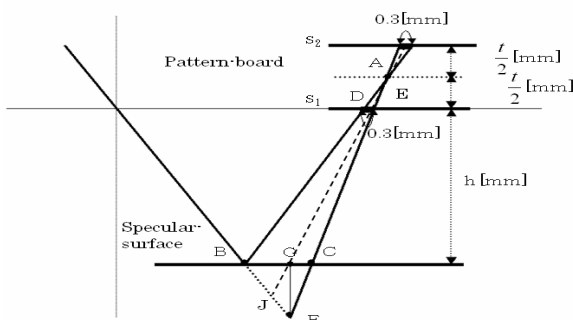

Figure 10.　The estimation of the quantization errors.

6 Conclusions

This paper has described a new approach for specular surface measurements, in which the range and shape of specular surfaces are obtained from virtual images of two pattern boards taken by a camera through the surfaces. Each reflection position on the surface can be located geometrically using the triangulation principle without any prior knowledge of the coordinates of other reflection points. One of the best features of our technique is that the detection principle is simple and does not contain ambiguity. Another feature is that it enables us to obtain a high spatial resolution of detection by using the phase shift technique.   The weak point is that the quantization error appears in detection results as mentioned above.

The presented approach paves the way for the inspection of specular surfaces, such as glass mirrors and polished metal as well as a specular ceramic material.

References

[1] Y.Nakagawa, Y.Oshida, T.Ninomiya and H.Sasaki: ”Shape detection of solder joints by spotlight scanning light-section method,” Trans.SICE, Vol.22, No.9, pp.982-987, 1986

[2] Sanderson A.C., Weiss L.E. and Nayer S.K.: ”Structured highlight inspection of specular sureface,” IEEE Trans.Patt.Anal.Machine Intell., PAMI-10, Vol.1, pp.44-55, 1988

[3] S.K.Nayar, A.C.Sanderson, L.E.Weiss and D.A.Simon: “Specular surface inspection using structured highlight and Gaussian images”, IEEE Trans. Robotics and Automation, Vol.6, No.2, pp.208-218, 1990

[4] T.Kuroda and H.Miike: “Measuring 3-D shape based on specular image processing with CG-based projection of pattern light source,” IEICE, Technical Report, IE96-69, 15-20, 1996

[5] T.Miyake, K.Yusuf and Y.Hongo: “Detection of specular surface normals and reconstruction of the shape,” IEICE Trans., Vol.J81-DII, No.7, pp.1556-1563, 1998

[6] T.Yoshizawa and K.Suzuki: “Automatic 3D measurement of shape by grating projection method,” JSPE, Vo.53, No.3, pp.66-70, 1987

[7] X.Ye, S.Fujimura and N.Yamada: “Measuring shape of glossy surface by using encoded grating illumination, “ Trans.SICE, Vol.26, No.11, pp.1313-1315, 1990

[8] T.Nishimura, S.Fujimura, T.Ito and S.Kiyasu: “Measurement of 3-D shape for glossy objects using M-array coded light source,” Trans.IEE, C, Vol.112, No.2, 97-101, 1992

[9] Z.Wang, H.Kato, K.Sato and S.Inokuchi: “Three dimensional measurement of specular objects”, IEICE Trans., Vol.J75-D-II, No.7, pp.1177-1186, 1992

[10] M.Yamamoto, M.Tonooka, Y.Otani and T.Yoshizawa: “Surface profile measurement of specular objects by grating projection method,” JSPE., Vol.64, No.8, pp.1171-1175, 1998

[11] M.Oshima, Y.Sato and M.Ito: “Specular surface measurement from pattern distortion,” Proc. Symp. on Sensing via Image Information (SSII2000), F-1, pp.223-226, 2000

[12] S.Savarese, M.Chen and P.Perona: “Recovering local shape of a mirror surface from reflection of a regular grid,” ECCV2004, LNCS 3023, pp.468-481, 2004

[13] W.S.Ching, P.S.Toh, K.Luk and M.Hwa: “Robust vergence with concurrent detection of occlusion and specular highlights,” Proc. Int. Conf. Comp. Vision, pp.384-394, 1993

[14] A.Blake: “Specular stereo,” Proc. Int. Join. Conf. Intel. Artif., pp.973-976, 1985

[15] D.N.Bhat and S.K.Nayar: “Stereo and specular reflection,” Int. Journ. Comp. Vision,” Vol.26, No.2, pp.91-106, 1998

[16] M.Oren and S.K.Nayer: “A theory of specular sureface geometry,” Inter.J ourn. Compt. Vis., Vol.24, No.2, pp.105-124, 1996

[17] K.Koshikawa and Y.Shirai: “A model   based recognition of glossy objects using their polarimetric properties,” Adv. Robot, Vol.2, No.2, pp.137-147, 1987

[18] L.B.Wolff and T.E.Boult: “Constraining object features using a polarization relectance model,” IEEE Trans. Patt. Anal. Mach. Intel., Vol.13, No.7, pp.635-657, 1991